Journal of Luminescence 211 (2019) 48–53

Contents lists available at ScienceDirect

Journal of Luminescence

journal homepage: www.elsevier.com/locate/jlumin

Variation of the conduction band edge of $(Lu,Gd)_3(Ga,Al)_5O_{12}$:Ce garnets studied by thermally stimulated luminescence

V. Khanin[a,b,*], I. Venevtsev[c], K. Chernenko[c,e], P. Rodnyi[c], T. van Swieten[a], S. Spoor[b], J. Boerekamp[b], H. Wieczorek[b], I. Vrubel[d], A. Meijerink[a], C. Ronda[b]

[a] Utrecht University, Princetonplein 5, 3584 CC Utrecht, the Netherlands
[b] Philips Research, High Tech Campus 34, 5656 AE Eindhoven, the Netherlands
[c] Peter the Great St. Petersburg Polytechnic University, Polytekhnicheskaya 29, 195251 St.Petersburg, Russia
[d] ITMO University, Kronverksky 49, 197101 St.Petersburg, Russia
[e] MAX IV Laboratory, Lund University, SE-22100 Lund, Sweden

ARTICLE INFO

Keywords:
Thermally stimulated luminescence
Complex garnets
Impurity-related traps
Thermal trap depth

ABSTRACT

The shift of the conduction band (CB) edge for thirty different $(Lu,Gd)_3(Ga,Al)_5O_{12}$:Ce compositions, with simultaneous variation in Lu/Gd and Ga/Al content was studied using thermally stimulated luminescence (TSL). Specific TSL peaks were related to impurities of Ta, Cr, Yb, Ti and Eu in $Lu_1Gd_2Ga_3Al_2O_{12}$:Ce ceramics. The shift of Yb-related peak positions (in temperature and trap depth) with composition modification was investigated as well. In Gd-containing $(Lu,Gd)_3(Ga,Al)_5O_{12}$ compositions a non-monotonous shift of the CB edge with increasing Ga content has been affirmed. The difference between thermal trap depths evaluated from our TSL experiments and optical trap depths obtained from the literature was explained by the role of lattice relaxation.

1. Introduction

Multicomponent garnets with the general formula $(Lu,Gd)_3(Ga,Al)_5O_{12}$:Ce are of interest as potential scintillators [1] or persistent phosphors [2] in view of the versatility of their composition that enables tuning of luminescence properties towards application requirements. Substitution (partial or complete) of Lu and Al ions by Gd and Ga ions, respectively, allows shifting the Ce^{3+} emission wavelength [3], the thermal stability of Ce^{3+} luminescence [4,5] and defect energy level positions [6] (and thus adjusting luminescence decay [7] and afterglow behavior [8]).

Changes in the conduction band (CB) edge with $(Lu,Gd)_3(Ga,Al)_5O_{12}$:Ce composition are the main reasons for variation in garnet afterglow characteristics [9,10]. The CB edge is formed by 5 d orbitals of lanthanide ions and 4p, 4s orbitals of Ga ions [11] and with composition variation its energy-position shifts strongly. The energy gap between the $5d_1$ Ce^{3+} band and the CB edge influences the thermal stability of luminescence [5], while the energy depth of defect levels heavily affects the afterglow dynamics [12,13].

Thermally stimulated luminescence (TSL) glow curves have been utilized to estimate the shift of the band edge of various materials [14–16]. For garnets doped with Ce^{3+} it has been reported [10,13,17] that their TSL glow curve structure is due to trapping of electrons at various defects followed by recombination on Ce^{3+} via thermal detrapping to the CB [18]. This process has been used to probe the shift of the CB edge of $Lu_3(Ga,Al)_5O_{12}$:Ce [10] and $Y_3(Ga,Al)_5O_{12}$:Ce [19–21]. It has been found that in $Lu_3(Ga,Al)_5O_{12}$:Ce, the CB edge shifts to lower energy monotonously with increasing substitution of Al by Ga [10].

However, in $Y_3(Ga,Al)_5O_{12}$:Ce with introduction of small (< 20%) Ga concentration to YAG, the CB edge position increases in energy (relative to the valence band, VB). While with further substitution of Al with Ga ions in $Y_3(Ga,Al)_5O_{12}$:Ce lattice the CB edge decrease in energy. The effects have been assigned to crystal field (CF) influence on 4 d orbitals of Y (movement of CB edge up) combined with contribution to CB edge states from Ga 4s, 4p orbitals (movement of CB edge down) [11].

DFT investigations [22] have resulted in the following picture for $(Lu,Gd)_3(Ga,Al)_5O_{12}$: the CB bottom shifts to lower energy (relative to the VB) monotonously with increasing Ga content in $Lu_3(Ga,Al)_5O_{12}$, but introduction of Gd in the $Lu_{3-x}Gd_x$ $(Ga,Al)_5O_{12}$ for $x > 0.5$ results in a non-monotonous shift of the CB with Ga/Al variation.

In this work we present experimental evidence of CB edge shift throughout the full range of $(Lu,Gd)_3(Ga,Al)_5O_{12}$:Ce compositions (from Lu to Gd and from Al to Ga simultaneously) with TSL glow curve measurements. We do this based on variation in positions of TSL peaks related to Yb trace impurity of which we systematically track the shift

* Corresponding author. Utrecht University, Princetonplein 1, 3584 CC Utrecht, the Netherlands.
E-mail address: khanin.vasilii@mail.ru (V. Khanin).

https://doi.org/10.1016/j.jlumin.2019.03.013
Received 7 December 2018; Received in revised form 5 March 2019; Accepted 7 March 2019
Available online 08 March 2019
0022-2313/

Table 1
Impurity-related (Cr, Yb, Ti) TSL peak maxima depending on the composition of the (Lu_yGd_{3-y}) $(Ga_xAl_{5-x})O_{12}$:Ce ceramics. The empty cells are due to low resolution of the TSL peaks for some of the compositions.

Lu, x	Ga, y	T_{max}^{Cr}, K	T_{max}^{Yb}, K	T_{max}^{Ti}, K	Lu, x	Ga, y	T_{max}^{Cr}, K	T_{max}^{Yb}, K	T_{max}^{Ti}, K
0	3	255	320	334	1.04	2	319	367	
0	4	294	358	434	1.04	3	255	302	371
0	2	290	354	430	1.04	3	256	304	383
0	1		357	435[a]	1.04	2.5	277	345	392
0.26	2	302	354	421	1.04	2	315	368	459
0.28	2	302	353	421	1.04	4	183	235[a]	340
0.32	2	312	360	421	1.04	1	335	382	434
0.34	2	307	357	414	1.04	0	318	368	422
0.34	2	293	347	420	1.04	3	255	307	384
0.34	2.5	290	337	412	1.05	3	255	310	390
0.34	2.5	285	337		1.06	2	320	364	
0.36	2	310	360	421	1.07	3	259	303	
0.36	2.5	278	325		3.04	1		449[a]	502
1.03	2.5	291	343		3.04	0	522[a]	567[a]	
1.04	2	320	376	428	3.04	3	261	317	
1.04	2	310	360	441	3.04	2		403	

[a] Tentative assignments.

of their position (in temperature and trap depth) with composition. Recently, it has been experimentally shown with transmission spectroscopy that in $Y_3Ga_3Al_2O_{12}$:Ce,Yb, Yb^{3+} acts as trap by capturing an electron in its 4f shell [23], which is well shielded from the environment by filled $5s^2$ and $5p^6$ orbitals. Thus, in this work additional attention is given to TSL peaks related to $Yb^{3+/2+}$ as it allows to connect the energy trap depth to the vacuum referred binding energy (VRBE) diagrams [9].

2. Experimental

Garnet ceramic $(Lu,Gd)_3(Ga,Al)_5O_{12}$:Ce 0.2 mol.% samples were prepared at Philips Research Eindhoven by sintering a mixture of base oxides of 4N-purity in air atmosphere in the form of disks of 14 mm diameter and 1 mm thickness. The compositions are listed in Table 1. Additionally, $Lu_1Gd_2Ga_3Al_2O_{12}$:Ce 0.2 mol.% ceramics with 25 wt. ppm Me-oxide co-doping, where Me = Ta, Ti, Cr, Yb or Eu, have been sintered. Based on X-ray diffraction patterns it was concluded that all samples consist of a single garnet phase.

TSL glow curves were measured in the 80–550 K temperature range after irradiation of the samples with X-rays (40 kV, 10 mA, tungsten anode, 3 cm away from the sample) at 80 K. The detector was a Hamamatsu R6357 PMT, sensitive in the range of 200–900 nm. The samples were glued to the heating element with Leitsilber-200 paint to ensure good thermal contact. The waiting time between irradiation of the samples and the start of the measurements was 10 min. The TSL curves shown in this paper were recorded with β = 15 K/min heating rate.

TSL glow curves after UV irradiation have been measured also in the 300–750 K temperature range with β = 15 K/min heating rate after illumination of the samples with Osram 450 W Xe arc lamp for 100 s. The light was directed through a monochromator inside an Edinburgh Instruments spectrofluorometer UC-920 at 365 nm with all slits between the lamp and the sample set to 10.0 mm. The waiting time between illumination of the samples and the start of the measurements was 5 min.

3. Results

In Fig. 1 the TSL glow curves for $Lu_1Gd_2Ga_3Al_2O_{12}$:Ce garnet ceramics without any additional co-doping (curve 1) and with various co-dopants (curves 2–6) are shown. Let us consider the origins of the observed TSL glow peaks.

The TSL curve of $Lu_1Gd_2Ga_3Al_2O_{12}$:Ce ceramics without an additional intentional co-dopant (Fig. 1, curve 1) consists of several TSL

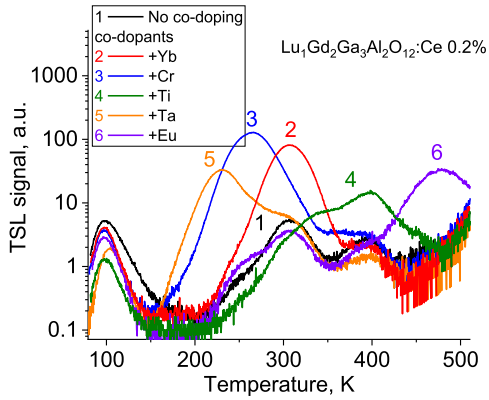

Fig. 1. TSL glow curves of non-intentionally doped $Lu_1Gd_2Ga_3Al_2O_{12}$:Ce garnet ceramics (1) or co-doped with 25 wt. ppm of the metal oxides: Yb (2) and Eu (6) rare-earth oxides and Cr (3), Ti (4) and Ta (5) transition metal oxides.

peaks: at 100, 250, 303 and 390 K. The apparent 100 K peak is actually part of a complex TSL structure in the range of 4–150 K [24], partially beyond the limit of our equipment (the lowest temperature we can reach corresponds to the boiling temperature of N_2, 77 K). The low-temperature TSL peaks are sensitive to stoichiometry distortions [8,20] and are usually assigned to surface [25] or bulk [26,27] structural point defects of various origin [25,28–30], which form shallow electron traps just below the edge of CB.

Deeper traps in garnets are associated with various impurities [2,31–33]. In Ref. [20] it was shown that the 303 K TSL peak for $Lu_1Gd_2Ga_3Al_2O_{12}$:Ce, Yb composition is associated with an Yb-impurity, see also Fig. 1, curve 2. It has been reported for various oxide garnets [12,34] that the two TSL peaks on either side of the Yb-related peak are also due to trace impurities. Intentional co-doping $Lu_1Gd_2Ga_3Al_2O_{12}$:Ce, Me with Me = Cr, Ti ions yields that 256 K peak is related to Cr and 390 K peak is related to Ti impurities (Fig. 1, curves 3 and 4). Doping with Ta and Eu ions results in TSL peaks at 230 and 480 K, respectively (see Fig. 1, curves 5 and 6). Intentional co-doping with impurities changes or increases (note the logarithmic scale in Fig. 1) the intensity of only one specific TSL peak, different for each impurity [34]. While the remainder of the TSL glow curves structure stays virtually the same.

Having identified the impurities responsible for specific TSL peaks we can trace their shift with temperature to discuss the dependence of CB energy position on $(Lu,Gd)_3(Ga,Al)_5O_{12}$:Ce composition modifications.

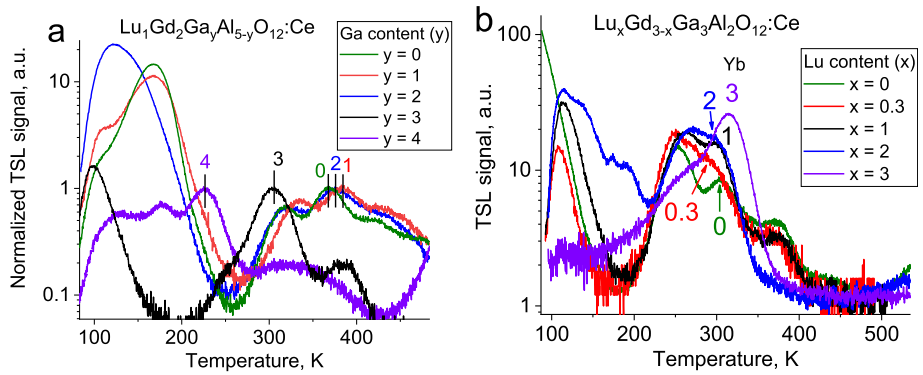

Fig. 2. a) Normalized TSL glow curves for $Lu_1Gd_2(Ga_yAl_{5-y})O_{12}$:Ce with varying Ga (y) content $0 \le y \le 4$, and b) TSL glow curves for $(Lu_xGd_{3-x})Ga_3Al_2O_{12}$:Ce with varying Lu (x) content $0 \le x \le 3$.

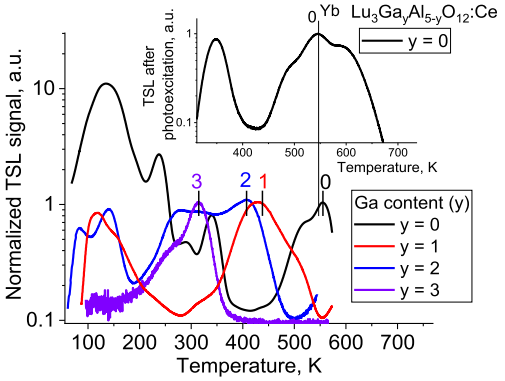

Fig. 3. Normalized TSL glow curves for $Lu_3Ga_yAl_{5-y}O_{12}$:Ce compositions. The vertical lines mark the Yb-related impurity. The inset shows the high-temperature TSL glow curve for LuAG:Ce ceramics illuminated at RT with a Xe lamp at 450 nm.

Fig. 2a shows the dependence of the TSL glow curves on the Ga (y) content in $Lu_1Gd_2(Ga_yAl_{5-y})O_{12}$:Ce ceramics ($0 \le y \le 4$). The TSL curve for $Lu_1Gd_2(Ga_yAl_{5-y})O_{12}$:Ce with y = 3 (curve 3) is the same as the reference curve in Fig. 1 (curve 1). For low Ga content (approximately till $y \approx 2$), addition of Ga ions in the Al-garnet lattice of $(Lu_1Gd_2)Al_5O_{12}$:Ce leads to the shift of the TSL peak to higher temperature and with further substitution of Al ions by 60–80% of Ga ions (y = 3, 4) the TSL peak gradually shifts to lower temperatures. The lowest Yb-related TSL peak position (for ceramics with y = 4, curve 4) is tentatively assigned as 235 K. The garnets containing 100% Ga show no Ce emission in the temperature range above 100 K [13], therefore, the measurements were carried out for garnets with Ga content up to 80%.

The TSL glow curves shape for many $(Lu,Gd)_3(Ga,Al)_5O_{12}$:Ce compositions is the same, but shifted in temperature, due to the variation in energy distance between trap levels and CB edge. The observed (Fig. 2a) small changes in high-temperature peak intensities are the consequence of variation in trace impurities originating from raw oxides. One can compare curve "y = 3" with the others from Fig. 2a: the TSL glow curves for y = 0, 1, 2 have the same shape, but it is the different for y = 3. The difference is due to the use of another Ga_2O_3 oxide for sintering of "y = 3" sample, leading to variation in transition metal impurities and subsequent change in related TSL peak intensities – namely 255 K (Cr-related) and 390 K (Ti-related).

The dependence of the TSL glow curves on the Lu (x) content in the $(Lu_xGd_{3-x})Ga_3Al_2O_{12}$:Ce, $x = 0 \div 3$ ceramics is depicted in Fig. 2b. The TSL curve of $Gd_3(Ga_3Al_2)O_{12}$:Ce (x = 0) sample consists of four peaks at 100, 255, 305 and 390 K. Again, the apparent 100 K peak is part of a complex TSL structure in the range of 4–150 K [24], partially beyond the limit of our equipment. The Cr-related TSL peak is encountered at around 255 K. The deeper traps belong to Yb (305 K) and Ti (390 K) impurities, respectively.

Gradual substitution of Gd ions with Lu ones does not change the TSL glow curve structure of $(Lu_xGd_{3-x})Ga_3Al_2O_{12}$:Ce strongly. The only significant change observed is the appearance of an additional TSL peak at 300–320 K with increasing Lu content. The connection of this new TSL peak with the Yb-impurity has been shown in Refs. [31,33]. Please note that curve "x = 1" in Fig. 2b is obtained for the same composition (but different set of raw materials batches) as curve 1 in Fig. 1, in which the connection of 303 K peak with Yb co-doping is clear. Yb^{3+} is a common impurity for Lu-based materials (these two elements are next to each other in the periodic table and separating them is a challenge) [35,36], and thus the appearance of the Yb-related TSL peak with increasing Lu content in $(Lu_{3-y}Gd_y)$, $(Ga_3Al_2)O_{12}$:Ce garnets is to be expected.

It is interesting that full substitution of Gd^{3+} by Lu^{3+} in Fig. 2b leads to a shift of 20 K of the Yb-related TSL peaks (300–320 K), while Cr-related TSL peaks (256 K) do not change their position within the experimental error margins.

The dependence of TSL glow curves on Ga content for $Lu_3(Ga_yAl_{5-y})O_{12}$:Ce garnets is shown in Fig. 3. The glow curve with y = 3 (Fig. 3 curve 3) is the same as curve "x = 3" in Fig. 2b (the colors are consistent), for which we have established the relation of the Yb impurity with the 320 K peak. We trace the shift of the TSL peak maxima for the Yb-related peak in Lu-garnets, marked with a vertical line, Fig. 3.

Fig. 3 shows a monotonous shift of the TSL glow curve structure to lower temperatures with increasing Ga content for $Lu_3(Ga_xAl_{5-x})O_{12}$:Ce, in line with previous findings [10]. The inset in Fig. 3 shows the TSL glow curve for LuAG:Ce ceramics expanded to higher temperature, excited at RT under Xe-lamp 450 nm illumination. The same triple-structure related to Cr (510 K), Yb (567 K) and Ti (615 K) impurities in LuAG:Ce with 50–60 K in between the peaks has been observed in Fig. 2a for $Lu_1Gd_2(Ga_xAl_{5-x})O_{12}$:Ce in the 250–400 K temperature range. The difference in the temperature range in which the impurity-related peaks are observed in $Lu_1Gd_2(Ga_yAl_{5-y})O_{12}$:Ce and LuAG:Ce is due to larger band gap for LuAG [6,10]. The CB edge position (compared to VRBE [9]) of LuAG is much higher than that for $Lu_1Gd_2(Ga_yAl_{5-y})O_{12}$, thus the impurity-related trap levels are significantly deeper in the band gap.

The TSL data are summarized in Table 1 for Yb, Cr and Ti-related impurities wherever possible. The values obtained for TSL peaks related to Yb-impurity are used in the next section to estimate the shift of the CB edge with composition variation.

4. Discussion

The values obtained for the TSL peak maxima and respective trap depths (see below) allow us to trace the position of the CB edge in complex garnets of variable composition. We use Yb-related TSL peak

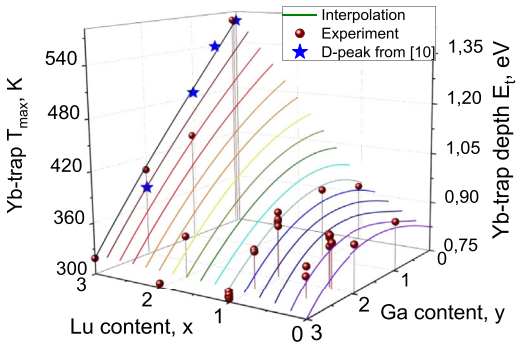

Fig. 4. TSL peak maxima for Yb-related trap as a function of (Lu_xGd_{3-x}) $(Ga_yAl_{5-y})O_{12}$:Ce composition. Dots – experimental data from Table 1, lines – interpolation towards other compositions. The right y-axis indicates the calculated thermal trap depth (E_t) for Yb-related traps, using eq. (1).

positions and trap depths, as other impurity related peaks (Cr and Ti) are co-dependent on the chemical environment, as the crystal field splitting affects the energy of the 3 d-states in which electrons are trapped. For lanthanide ions which trap electrons in the 4f-orbital (as is the case for Yb^{3+} [23]) the VRBE is independent of the crystal field.

In our calculation of the thermal trap depth (E_t) from TSL peak positions we have used our previous findings [12,20] as well as literature evaluations [13,33,37] showing that impurity-related traps in garnets have a nearly constant frequency factor (s) in the order of $s = 10^{12 \pm 1}\ s^{-1}$. A small modification of the Urbach empirical method (correcting for differences in frequency factor and heating rate) gives us a simple formula eq. (1) to estimate E_t [38]:

$$E_t = 29kT_{max} \approx \frac{T_{max}}{400}\ [eV], \quad (1)$$

where E_t is the thermal trap depth (eV); k is the Boltzmann constant (eV/K) and T_{max} is the TSL peak maximum (K).

The estimated trap depths from the TSL peak maxima positions (Table 1) of the Yb-related defect in (Lu_xGd_{3-x}) $(Ga_yAl_{5-y})O_{12}$:Ce ceramics are plotted in Fig. 4. Assuming smooth changes in the band gap between different compositions, we interpolate the trap depth of the Yb-related trap to other compositions for Lu $0 \le x \le 3$ and Ga $0 \le y \le 3$. The graph shows the dependence of Yb-trap depths on garnet composition and we use it to evaluate the CB edge changes with Lu/Gd and Al/Ga variation. The data for $Lu_3Ga_yAl_{5-y}O_{12}$:Ce row is rather limited, but additional data points have been obtained from Ref. [10], describing the changes of D-peak in $Lu_3(Ga_xAl_{5-x})O_{12}$:Ce with Ga/Al substitution as "stars", Fig. 4. The "star"-data point for LuAG:Ce [10] is normalized to our data point (x = 3, y = 0).

Fig. 4 also depicts the reproducibility of the sample preparation, e.g. data points belonging to two nominally pure LuAG:Ce samples (no Ga or Gd present) in the top left corner of the graph give very similar values of 567 and 569 K for the Yb-related TSL peak maxima. The precision of the TSL measurements is ± (3–5) K. Some other dots show the variation of TSL peak maxima with stoichiometry distortions (z) such as $Lu_1Gd_{2-z-0.06}Ga_{2+z}Al_3O_{12}$:$Ce_{0.06}$, where $|z| \le 0.05$. The control of the exact stoichiometry of the final ceramic sample is a difficult process [39] and some spread in the data can be observed (Fig. 4), indicated by more than one data point belonging to the same nominal composition.

The main feature of Fig. 4 is the non-monotonous change of the Yb-trap TSL peak maxima with Ga-content for garnets containing Gd, while for Lu-garnets the trap depths become monotonously shallower with increasing Ga content.

The thermal trap depth (E_t) for the Yb-related peak is the difference between the CB edge and the energy level of the defect itself. For $Y_3(Ga,Al)_5O_{12}$:Ce, Yb it has been experimentally shown with transmission spectroscopy that $Yb^{3+/2+}$ itself acts as a trap [23]. As the electron is captured into the Yb^{3+} ions' 4f shell, which is shielded from surrounding ligands, the shift of the Yb thermal trap depth (E_t) probes the CB band edge and its shift relative to VRBE [9].

A non-monotonous shift of the CB edge has been observed experimentally for $Y_3(Al,Ga)_5O_{12}$:Ce [20,21,34] and theoretically for $(Lu,Gd)_3(Al,Ga)_5O_{12}$:Ce [22] garnets and has been rationalized by DFT-calculations [11]: the DFT calculations show a variation in orbitals that contribute to the edge of the CB. On the other hand, $Lu_3(Al,Ga)_5O_{12}$ garnets have been shown and calculated to have the usual monotonous shift of the CB with composition variation [10]. All these findings are consistent with the data shown in Fig. 4.

The CB edge of $RE_3Al_5O_{12}$, RE = Lu, Y, Gd is formed by 5 d orbitals of the RE ion [22] (4 d in case of Y-garnet [40]), though the energy position of the orbitals is rather different when compared to vacuum level [9]. The effect of Ga/Al substitution on CB edge formation is the same for Y-, Lu- and Gd-garnets, but in Lu-garnets the Al 3s,p orbitals are very close in energy to the CB edge [22]. Conceivably, minimal addition of Ga into $Lu_3(Ga,Al)_5O_{12}$ lattice (and with Lu 5 d orbital sequent shift-up in energy) immediately leads to CB edge being formed by Al 3s,p orbitals [11]. The integer variation (x = 0:1) in Ga/Al content of our experiment is too large a step to sample a potential non-monotonous shift of $Lu_3(Ga_xAl_{5-x})O_{12}$ band gap for low values of x.

After having calculated the thermal trap depths (E_t), we can now construct the respective band diagrams and compare them with literature data for $Lu_3(Al,Ga)_5O_{12}$ and $Gd_3(Al,Ga)_5O_{12}$ [9] obtained with photoionization experiments (E_{opt}), see Table 2 and Fig. 5a.

The Y-axis of the diagram in Fig. 5a is based on VRBE [9] with addition of thermal trap depth E_t from Table 2. The error margins for $Yb^{2+/3+}$ optical depth are reported [9] to be ± 0.1 eV, while our estimations show similar precision of ± 0.1 eV for E_t-values because of uncertainty in TSL peak maxima T_m, K and frequency factor s, s^{-1} evaluation. The difference between E_{opt}-values from Ref. [9] and E_t data from Table 2 is significant (~0.4 ÷ 0.5 eV), and it is nearly constant.

The systematic difference of ~ 0.5 eV between optical and thermal trap depths has been observed for various dosimetry and scintillation materials [41–43]. During optical excitation the lattice does not relax, whereas thermal excitation connects the completely relaxed ground state to the completely relaxed excited state. Consequently, the optical trap depth is larger than the thermal trap depth, the difference being the lattice relaxation energy. The relaxation energy is due to the lattice response (changing metal-ligand distances) on changing the charge of the trap. This is depicted in Fig. 5b. The optical trap depths determined from maxima in absorption spectra correspond to the minimum energy required to place an electron originating from Yb^{2+} in the conduction band, while not changing the metal-ligand distances (Born-Oppenheimer approximation). This leaves the resulting Yb^{3+} ion in a non-relaxed state, immediately after the optical transition, followed by

Table 2
Thermal $Yb^{3+/2+}$ -trap depths (E_t) presented in Fig. 4 and photoionization energies (optical depth E_{opt}) of $Yb^{3+/2+}$ in some of the $Lu_3(Al,Ga)_5O_{12}$ and $Gd_3(Al,Ga)_5O_{12}$ garnets gathered by Dorenbos [9]. ΔE is the difference between the optical and thermal trap depth.

$Lu_3(Al,Ga)_5O_{12}$:CeGa	E_t, eV	E_{opt}, eV [9]	$E_{opt} - E_t = \Delta E$, eV
0	1.42	1.85	0.44
1	1.08	1.59	0.51
2	1.01	1.46	0.46
3	0.79	1.20	0.41
$Gd_3(Al,Ga)_5O_{12}$:CeGa	E_t, eV	E_{opt}, eV [9]	ΔE, eV
1	0.89	1.30	0.41
2	0.88	1.32	0.44

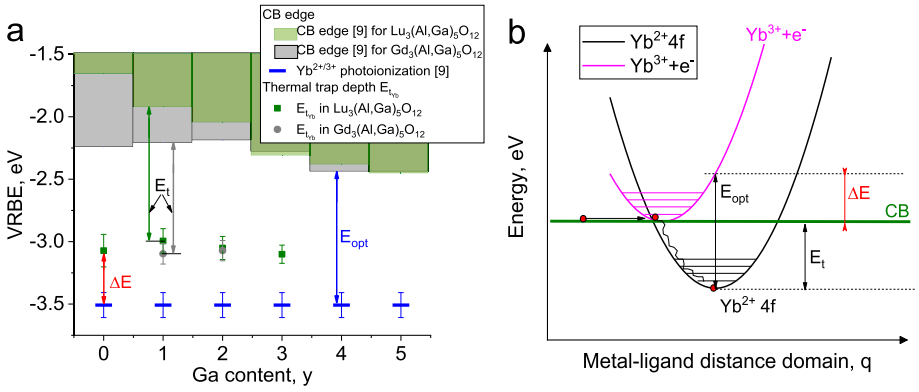

Fig. 5. (a) Band gap diagram constructed on VRBE scale for $Lu_3(Al,Ga)_5O_{12}$ and $Gd_3(Al,Ga)_5O_{12}$ garnets showing comparison of optical (E_{opt}) and thermal (E_t) trap depth for $Yb^{2+/3+}$ comprised together from literature data [9] and our TSL experiments, respectively. (b) Configuration coordinate diagram for Yb^{2+} ($4f^{14}$) and $Yb^{3+}+e^-$ states relative to the conduction band.

thermal relaxation to the equilibrium distance in the new situation (a smaller distance for the situation depicted in Fig. 5b). As the metal-ligand distance is mainly determined by Yb (in its two valence states) and the ligands remain the same (oxygen ions), the relaxation energies in the different garnet compositions are not expected to vary significantly. This is in agreement with the findings in Table 2, in which we observe that the difference between thermal and optical trap depth (ΔE) is about 0.44 ± 0.07 eV.

5. Conclusions

We have shown that intentional co-doping of $Lu_1Gd_2Ga_3Al_2O_{12}$:Ce ceramics with impurities (Ta, Cr, Yb, Ti, Eu) gives rise to specific TSL peak, different for each co-dopant, while the rest of the glow curve structure stays virtually the same. Then we have systematically traced the shift of Yb-related peak position (in temperature and trap depth) with Ga/Al and Lu/Gd substitution in $(Lu,Gd)_3(Ga,Al)_5O_{12}$:Ce, which allows us to pinpoint the position of the CB edge for all compositions investigated.

Experimental evidence for the theoretically predicted [22] monotonous and non-monotonous shift of the CB edge depending on $(Lu,Gd)_3(Ga,Al)_5O_{12}$:Ce composition has been presented with evaluation of TSL measurements for Yb-related traps. The Yb-related trap depths (E_t) probe the CB band edge and its shift relative to the vacuum level (VRBE). A continuous shift to lower energies is observed for the CB-edge upon Ga-substitution in $Lu_3(Al,Ga)_5O_{12}$ while an initial shift to higher energies followed by a shift to lower energies is demonstrated for $Gd_3(Al,Ga)_5O_{12}$. Finally, differences between trap depths determined from photoionization experiments for $Yb^{2+/3+}$ [9] and thermal Yb-trap depths have been reported and shown to be constant, which is expected as the lattice relaxation is mainly governed by the change in Yb-oxygen distance which is expected to be similar in the garnet hosts.

References

[1] J. Luo, Y. Wu, G. Zhang, H. Zhang, G. Ren, Composition–property relationships in (Gd3− xLux)(GayAl5−y) O12: Ce (x= 0, 1, 2, 3 and y= 0, 1, 2, 3, 4) multi-component garnet scintillators, Opt. Mater. 36 (2013) 476–481.

[2] J. Ueda, K. Kuroishi, S. Tanabe, Bright persistent ceramic phosphors of Ce3+-Cr 3+-codoped garnet able to store by blue light, Appl. Phys. Lett. 104 (2014).

[3] J. Ueda, Analysis of optoelectronic properties and development of new persistent phosphor in Ce3+-doped garnet ceramics, J. Ceram. Soc. Japan 123 (2015) 1059–1064.

[4] Q. Shao, Y. Dong, J. Jiang, C. Liang, J. He, Temperature-dependent photoluminescence properties of (Y, Lu) 3Al5O12: Ce3+ phosphors for white LEDs applications, J. Lumin. 131 (2011) 1013–1015.

[5] J.M. Ogiegło, A. Katelnikovas, A. Zych, T. Jüstel, A. Meijerink, C.R. Ronda, Luminescence and luminescence quenching in Gd3(Ga,Al) 5O12 scintillators doped with Ce3+, J. Phys. Chem. A 117 (12) (2013) 2479–2484, https://doi.org/10.1021/jp309572p.

[6] M. Nikl, K. Kamada, V. Babin, J. Pejchal, K. Pilarova, E. Mihokova, A. Beitlerova, K. Bartosiewicz, S. Kurosawa, A. Yoshikawa, Defect engineering in Ce-doped aluminum garnet single crystal scintillators, Cryst. Growth Des. 14 (2014) 4827–4833.

[7] K. Kamada, T. Yanagida, J. Pejchal, M. Nikl, T. Endo, K. Tsutumi, Y. Fujimoto, A. Fukabori, A. Yoshikawa, Scintillator-oriented combinatorial search in Ce-doped (Y, Gd) 3 (Ga, Al) 5O12 multicomponent garnet compounds, J. Phys. D Appl. Phys. 44 (2011) 505104.

[8] T. Kanai, M. Satoh, I. Miura, Characteristics of a nonstoichiometric Gd3+ δ (Al, Ga) 5− δO12: Ce garnet scintillator, J. Am. Ceram. Soc. 91 (2008) 456–462.

[9] P. Dorenbos, Electronic structure and optical properties of the lanthanide activated RE3 (Al1− xGax) 5O12 (RE= Gd, Y, Lu) garnet compounds, J. Lumin. 134 (2013) 310–318.

[10] B.P. Uberuaga, C.R. Stanek, M. Fasoli, D.A. Andersson, A. Vedda, K.J. McClellan, M. Nikl, C. Jiang, Band-gap engineering for removing shallow traps in rare-earth Lu 3 Al 5 O 12 garnet scintillators using Ga 3+ doping, Phys. Rev. B 84 (2011).

[11] I.I. Vrubel, R.G. Polozkov, I.A. Shelykh, V.M. Khanin, P.A. Rodnyi, C.R. Ronda, Bandgap engineering in yttrium-aluminum garnet with Ga doping, Cryst. Growth Des. 17 (2017) 1863–1869.

[12] V. Khanin, I. Venevtsev, S. Spoor, J. Boerekamp, A.M. van Dongen, H. Wieczorek, K. Chernenko, D. Buettner, C. Ronda, P. Rodnyi, A new method for unambiguous determination of trap parameters from afterglow and TSL curves connection: example on garnets, Opt. Mater. 72 (2017) 161–168.

[13] J. Ueda, P. Dorenbos, A.J.J. Bos, K. Kuroishi, S. Tanabe, Control of electron transfer between Ce 3+ and Cr 3+ in the Y 3 Al 5− x Ga x O 12 host via conduction band engineering, J. Mater. Chem. C. 3 (2015) 5642–5651.

[14] A.H. Krumpel, A.J.J. Bos, A. Bessière, E. van der Kolk, P. Dorenbos, Controlled electron and hole trapping in YPO 4: Ce 3+, Ln 3+ and LuPO 4: Ce 3+, Ln 3+(Ln= Sm, Dy, Ho, Er, Tm), Phys. Rev. B 80 (2009) 85103.

[15] V.S. Levushkina, D.A. Spassky, E.M. Aleksanyan, M.G. Brik, M.S. Tretyakova, B.I. Zadneprovski, A.N. Belsky, Bandgap engineering of the LuxY1− xPO4 mixed crystals, J. Lumin. 171 (2016) 33–39.

[16] P. Dorenbos, A review on how lanthanide impurity levels change with chemistry and structure of inorganic compounds, ECS J. Solid State Sci. Technol. 2 (2013) R3001–R3011.

[17] N.G. Romanov, D.O. Tolmachev, A.S. Gurin, Y.A. Uspenskaya, H.R. Asatryan, A.G. Badalyan, P.G. Baranov, H. Wieczorek, C. Ronda, Dramatic impact of the giant local magnetic fields on spin-dependent recombination processes in gadolinium based garnets, Appl. Phys. Lett. 106 (2015) 262404.

[18] J. Ueda, P. Dorenbos, A.J.J. Bos, A. Meijerink, S. Tanabe, Insight into the thermal quenching mechanism for Y3Al5O12: Ce3+ through thermoluminescence excitation spectroscopy, J. Phys. Chem. C 119 (2015) 25003–25008.

[19] J. Ueda, P. Dorenbos, A.J.J. Bos, K. Kuroishi, S. Tanabe, Control of electron transfer between Ce3+ and Cr3+ in the Y3Al5-xGaxO12 host via conduction band engineering, J. Mater. Chem. C. 3 (2015) 5642–5651.

[20] V. Khanin, I. Venevtsev, P. Rodnyi, C. Ronda, Changes in trap parameters in various mixed oxide garnets, Radiat. Meas. 90 (2015).

[21] V. Laguta, Y. Zorenko, V. Gorbenko, A. Iskaliyeva, Y. Zagorodniy, O. Sidletskiy, P. Bilski, A. Twardak, M. Nikl, Aluminum and gallium substitution in yttrium and lutetium aluminum–gallium garnets: investigation by single-crystal NMR and TSL methods, J. Phys. Chem. C 120 (2016) 24400–24408.

[22] S.K. Yadav, B.P. Uberuaga, M. Nikl, C. Jiang, C.R. Stanek, Band-gap and band-edge engineering of multicomponent garnet scintillators from first principles, Phys. Rev. Appl. 4 (2015) 54012.

[23] J. Ueda, S. Miyano, S. Tanabe, Formation of deep electron traps by Yb3+ codoping leads to super-Long persistent luminescence in Ce3+-doped yttrium aluminum gallium garnet phosphors, ACS Appl. Mater. Interfaces 10 (2018) 20652–20660.

[24] W. Drozdowski, K. Brylew, M.E. Witkowski, A.J. Wojtowicz, P. Solarz, K. Kamada, A. Yoshikawa, Studies of light yield as a function of temperature and low temperature thermoluminescence of Gd3Al2Ga3O12: Ce scintillator crystals, Opt. Mater. 36 (2014) 1665–1669.

[25] A.A. Trofimov, M.R. Marchewka, L.G. Jacobsohn, Effects of sintering temperature on the microstructure and luminescence of LuAG: Pr ceramics, Radiat. Meas. 122 (2019) 34–39, https://doi.org/10.1016/j.radmeas.2019.01.005.

[26] C. Hu, S. Liu, Y. Shi, H. Kou, J. Li, Y. Pan, X. Feng, Q. Liu, Antisite defects in nonstoichiometric Lu3Al5O12: Ce ceramic scintillators, Phys. Status Solidi 252 (2015) 1993–1999.

[27] E. Mihokova, M. Nikl, J.A. Mareš, A. Beitlerova, A. Vedda, K. Nejezchleb, K. Blažek, C. D'Ambrosio, Luminescence and scintillation properties of YAG: Ce single crystal

and optical ceramics, J. Lumin. 126 (2007) 77–80.
[28] M. Nikl, A. Vedda, V.V. Laguta, Energy transfer and storage processes in scintillators: the role and nature of defects, Radiat. Meas. 42 (2007) 509–514.
[29] F.A. Selim, D. Solodovnikov, M.H. Weber, K.G. Lynn, Identification of defects in Y 3 Al 5 O 12 crystals by positron annihilation spectroscopy, Appl. Phys. Lett. 91 (2007) 104105.
[30] M. Nikl, E. Mihokova, J. Pejchal, A. Vedda, Y. Zorenko, K. Nejezchleb, The antisite LuAl defect-related trap in Lu3Al5O12: Ce single crystal, Phys. Status Solidi 242 (2005) R119–R121.
[31] V.M. Khanin, P.A. Rodnyi, H. Wieczorek, C.R. Ronda, Electron traps in Gd3Ga3Al2O12:Ce garnets doped with rare-earth ions, Tech. Phys. Lett. 43 (2017) 439–442.
[32] E.D. Milliken, L.C. Oliveira, G. Denis, E.G. Yukihara, Testing a model-guided approach to the development of new thermoluminescent materials using YAG: Ln produced by solution combustion synthesis, J. Lumin. 132 (2012) 2495–2504.
[33] F. You, A.J.J. Bos, Q. Shi, S. Huang, P. Dorenbos, Electron transfer process between Ce3+ donor and Yb3+ acceptor levels in the bandgap of Y3Al5O12 (YAG), J. Phys. Condens. Matter 23 (2011) 215502.
[34] J. Ueda, A. Hashimoto, S. Takemura, K. Ogasawara, P. Dorenbos, S. Tanabe, Vacuum referred binding energy of 3d transition metal ions for persistent and photostimulated luminescence phosphors of cerium-doped garnets, J. Lumin. 192 (2017) 371–375.
[35] M. Kubota, Determination of trace impurities in high purity lutetium oxide by neutron activation with aid of cation-exchange separation, J. Nucl. Sci. Technol. 11 (1974) 334–338.
[36] L.C. Chandola, P.P. Khanna, Determination of rare earth impurities in high purity lutetium oxide by X-ray fluorescence spectrometry, Indian J. Pure Appl. Phys. 25 (1987) 157–159.
[37] E. Mihóková, K. Vávrů, K. Kamada, V. Babin, A. Yoshikawa, M. Nikl, Deep trapping states in cerium doped (Lu, Y, Gd) 3 (Ga, Al) 5O12 single crystal scintillators, Radiat. Meas. 56 (2013) 98–101.
[38] V. Pagonis, G. Kitis, C. Furetta, Numerical and Practical Exercises in Thermoluminescence, Springer, New York, 2006, p. 13.
[39] Z.M. Seeley, N.J. Cherepy, S.A. Payne, Expanded phase stability of Gd-based garnet transparent ceramic scintillators, J. Mater. Res. 29 (2014) 2332–2337.
[40] A.B. Muñoz-García, L. Seijo, Structural, electronic, and spectroscopic effects of Ga codoping on Ce-doped yttrium aluminum garnet: first-principles study, Phys. Rev. B 82 (2010) 184118.
[41] A.J.J. Bos, N.R.J. Poolton, J. Wallinga, A. Bessière, P. Dorenbos, Energy levels in YPO4: Ce3+, Sm3+ studied by thermally and optically stimulated luminescence, Radiat. Meas. 45 (2010) 343–346.
[42] P. Dorenbos, Systematic behaviour in trivalent lanthanide charge transfer energies, J. Phys. Condens. Matter 15 (2003) 8417.
[43] R. Chen, V. Pagonis, Thermally and Optically Stimulated Luminescence: A Simulation Approach, John Wiley & Sons, 2011, p. 11.